Journal of Applied Electrochemistry **32**: 1119–1129, 2002.

Anodic oxidation of copper cyanide on graphite anodes in alkaline solution

J. LU, D.B. DREISINGER* and W.C. COOPER
*Department of Metals and Materials Engineering, University of British Columbia, Vancouver, BC, Canada, V6T 1N8 (*author for correspondence)*

Received 25 June 2001; accepted in revised form 5 June 2002

Key words: anodic oxidation, copper cyanide, cupric oxide, cyanate, graphite anodes

Abstract

The anodic oxidation of copper cyanide has been studied using a graphite rotating disc with reference to cyanide concentration (0.05–4.00 M), CN:Cu mole ratio (3–12), temperature (25–60 °C) and hydroxide concentration (0.01–0.25 M). Copper had a significant catalytic effect on cyanide oxidation. In the low polarization region (about 0.4 V vs SCE or less), cuprous cyanide is oxidized to cupric cyanide complexes which further react to form cyanate. At a CN:Cu ratio of 3 and $[OH^-] = 0.25$ M, the Tafel slope was about 0.12 V decade^{-1}. $Cu(CN)_3^{2-}$ was discharged on the electrode and the reaction order with respect to the predicted concentration of $Cu(CN)_3^{2-}$ is one. With increasing CN:Cu mole ratio and decreasing pH, the dominant discharged species shifted to $Cu(CN)_4^{3-}$. Under these conditions, two Tafel slopes were observed with the first one being 0.060 V decade^{-1} and the second one 0.17–0.20 V decade^{-1}. In the high polarization region (about 0.4 V vs SCE or more), cuprous cyanide complexes were oxidized to copper oxide and cyanate. Possible reaction mechanism was discussed.

1. Introduction

1.1. *Oxidation of copper cyanide*

1.1.1. *Background*

Much attention has been paid to the study of the electrochemical oxidation of CN^- to minimize the destruction of cyanide in metal electrowinning from cyanide solution or alternatively maximize the efficiency of the destruction of cyanide in effluent streams to meet environmental requirements [1–18]. Relatively less work has been done on the anodic oxidation of copper cyanide and the results are incomplete and conflicting. A solvent extraction-electrowinning process has been developed at the University of British Columbia to recover copper and cyanide from gold mining effluents [18]. In summary, copper cyanide is solvent-extracted using a guanidine-based extractant or a mixed strong base amine (LIX 79, XI 7980, XI78 from Henkel Co.), stripped with strong alkaline electrolyte and finally electrolysed in a membrane cell to produce copper metal and a bleed stream for cyanide recovery. The use of a membrane (Nafion®) in the copper electrowinning cell is necessary to prevent cyanide oxidation at the anode. Unfortunately, the use of a membrane is expensive and the membrane may be subject to mechanical damage by the growing metal deposit. To eliminate the use of a membrane, the possible inclusion of sulfite as a sacrificial species was tested in some proof-of-concept electrowinning experiments and was shown to be promising [19]. With sulfite addition, the cell chemistry becomes as follows:

$$Na_2Cu(CN)_3 + \tfrac{1}{2}Na_2SO_3 + NaOH \rightarrow Cu + 3NaCN + \tfrac{1}{2}Na_2SO_4 + \tfrac{1}{2}H_2O \quad (1)$$

Accordingly, the objective of the present research was to understand the anodic oxidation of copper cyanide and then limit the anodic consumption of cyanide by the use of the sulfite sacrificial species during electrowinning. This contribution summarizes the detailed study of the anodic behaviour of copper cyanide solutions. A previous study [20] reported on the anodic oxidation of sulphite. A final paper in this series will report on the anodic chemistry of the Cu^+–CN^-–SO_3^{2-}–OH^- system.

1.1.2. *Literature review*

The products and mechanism of cyanide oxidation depend mainly on pH, potential and concentration. As a pseudo-halogen, CN^- can be oxidized to $(CN)_2$:

$$2CN^- = (CN)_2 + 2e^- \quad E^\circ = -0.176 \text{ V vs SHE} \quad (2)$$

Under alkaline conditions, the reaction for the oxidation of cyanide is cyanate [2, 3]:

$$CN^- + 2OH^- = CNO^- + H_2O + 2e^- \quad E^\circ = -0.97 \text{ V vs SHE} \quad (3)$$

In neutral and weakly alkaline solutions (pH 7.0–11.7), cyanogen is the main cyanide oxidation product according to Reaction 2 [2, 7, 17]. Cyanogen can react subsequently with hydroxide in solution to give cyanate and cyanide:

$$(CN)_2 + 2OH^- = CNO^- + CN^- + H_2O \quad (4)$$

There are some reports on the anodic oxidation of copper cyanide, but most concern the products and phenomena of the electrolytic oxidation and are incomplete [4, 7–9, 11–13]. According to Dart et al. [8], copper deposition releases free cyanide at the cathode and the free cyanide is oxidized to cyanate at the anode. Drogen and Pasek [9] proposed a direct oxidation route (copper cyanide complexes are directly oxidized to cyanate with the release of cuprous ions). Tan et al. [11] reported that copper cyanide complexes are first oxidized to cyanate releasing cuprous ions, which are then oxidized to copper hydroxide.

Yoshimura and Katagiri et al. [5–7] measured the steady-state polarization curves at a platinum anode in cyanide solutions containing a very small amount of copper and found that the Tafel slope was about 0.158 V decade^{-1} in a low potential region, suggesting that a simple one-electron reaction was occurring at the electrode. It was assumed that all the copper exists in the form of $Cu(CN)_4^{3-}$ but with no check on the distribution of copper species. In fact, in the ranges of cyanide and copper concentrations studied a significant amount of copper exists in the form of $Cu(CN)_3^{2-}$ and so their assumption was in error. The calculated reaction order with respect to $Cu(CN)_4^{3-}$ was 0.9. It was thought that $Cu(CN)_4^{3-}$ was oxidized to $Cu(CN)_4^{2-}$. The following mechanism was proposed [7]:

$$Cu(CN)_4^{3-} \rightarrow Cu(CN)_4^{2-} + e^- \quad (5)$$

$$2Cu(CN)_4^{2-} \Leftrightarrow Cu_2(CN)_6^{2-} + 2CN^- \quad (6)$$

$$Cu_2(CN)_6^{2-} \rightarrow 2Cu(CN)_2^- + (CN)_2 \quad (7)$$

$$Cu(CN)_2^- + 2CN^- \rightarrow Cu(CN)_4^{3-} \quad (8)$$

$$(CN)_2 + 2OH^- \rightarrow CN^- + OCN^- + H_2O \quad (9)$$

However, no kinetic data are given for alkaline copper cyanide solutions. In alkaline solutions (pH 11.8–14), the reaction can be expressed by Reaction 3 and cyanate ion is not oxidized further.

Hine et al. [12] reported that copper exhibited a catalytic effect on cyanide oxidation on a PbO_2 coated anode. The Tafel slope for the oxidation of a solution containing 1 M NaCN and 0.3 M copper was 0.070–0.110 V decade^{-1} in the current density range 0.05–10 A dm^{-2}. It was thought that the oxidation of $Cu(CN)_3^{2-}$ to $Cu(OH)_2$ and CN^- was occurring.

Hwang et al. [13] studied the electrolytic oxidation of copper cyanide solution with CN:Cu mole ratios of 2.8 to 20 and at different pHs using a platinum anode. In strongly alkaline solution (pH > 12), they proposed the reaction sequence:

$$Cu(CN)_n^{(n-1)-} + 2nOH^- = Cu^+ + nCNO^- + nH_2O + 2ne^- \quad (10)$$

$$2Cu^+ + 2OH^- = Cu_2O + H_2O \quad (11)$$

$$Cu_2O + 2OH^- = CuO + 2H_2O + 2e^- \quad (12)$$

The authors postulated that in neutral or weakly alkaline or acidic solutions, the complex first dissociates to free cyanide and then cyanide ions are oxidized. However, if the anode and the cathode are separated, anodic oxidation will not occur because no free cyanide released from the cathode comes to the anode. From the above discussion, it is evident that there are incomplete and conflicting results on the anodic oxidation of copper cyanide in alkaline solution.

1.2. *Thermodynamics of copper cyanide*

Copper cyanide species undergo the following successive equilibrium steps:

$$Cu^+ + 2CN^- = CuCN_2^- \quad \log \beta_2 = 24 \text{ at } 25\ ^\circ\text{C [21]} \quad (13)$$

$$Cu(CN)_2^- + CN^- = Cu(CN)_3^{2-} \quad \log K_{2,3} = 5.3 \text{ at } 25\ ^\circ\text{C [21]} \quad (14)$$

$$Cu(CN)_3^{2-} + CN^- = Cu(CN)_4^{3-} \quad \log K_{3,4} = 1.5 \text{ at } 25\ ^\circ\text{C [21]} \quad (15)$$

$$HCN = H^+ + CN^- \quad \log K_a = 9.21 \text{ at } 25\ ^\circ\text{C [22]} \quad (16)$$

where β_2, $K_{2,3}$, $K_{3,4}$, and K_a are the equilibrium constants of Reactions 13–16, respectively.

Considering the above equilibrium reactions, the distribution of these species depends on pH, temperature, the total concentrations of copper and cyanide and the mass balances of cyanocuprate species described by the following equations:

$$[Cu]_{Total} = [Cu^+] + [Cu(CN)_2^-] + [Cu(CN)_3^{2-}] + [Cu(CN)_4^{3-}] \quad (17)$$

$$[CN]_{Total} = [CN^-] + [HCN] + 2[Cu(CN)_2^-] + 3[Cu(CN)_3^{2-}] + 4[Cu(CN)_4^{3-}] \quad (18)$$

The detailed discussion of the effects of pH, total copper and cyanide, temperature will be published in another paper [23]. At a CN:Cu mole ratio less than 3, the distribution of cyanocuprate species depends mainly on

the mole ratio of cyanide to copper. The dominant species are tricyanide and dicyanide. At a CN:Cu mole ratio of 3, almost all the copper exists in the form of tricyanide. At CN:Cu mole ratios greater than 3, the distribution of the copper-cyanide species depends not only on the mole ratio of cyanide to copper but also on the total copper concentration. At low total copper concentration, copper tricyanide decreases slowly with increasing CN:Cu mole ratio, but at high total copper concentration, tricyanide decreases greatly with increasing CN:Cu mole ratio. The free Cu^+ concentration is below about 10^{-20} M at a CN:Cu mole ratio > 3, so the effect of free Cu^+ on cyanide oxidation does not need to be considered. In this study, the experiments were conducted in a supporting electrolyte providing essentially constant ionic strength, and the activity coefficients for all copper cyanide species could be considered to be constant. It is reasonable to assume that the equilibrium constants do not vary at constant ionic strength. Using this approach, it is possible to predict the solution speciation as a function of the CN:Cu mole ratio, copper concentration and in electrochemical oxidation studies, and to determine the reaction order with respect to cyanocuprate species.

2. Experimental details

2.1. *Equipment*

Impregnated NE-150 graphite rod from National Electric Carbon Co. was used to make a graphite rotating disc. The graphite was machined to 4 mm diameter and surrounded tightly with a plastic shield with 10 mm diameter. Another sample of graphite having 25 mm diameter was fashioned as a rotating disc for the coulometric measurements.

The rotating disc electrode system was an EG&G PARC (model 636) electrode rotator. The potentiostats used were Solartron (model 1286) and PARC 273A Electrochemical Interface. An EG&G water-jacketed electrolytic cell was used. Argon gas was used to protect copper cyanide species from possible oxidation by air. A Cannon–Fenske routine viscometer (size 25) was used to measure the kinematic viscosity of the solutions studied. Leybold Max 200 XPS instrument was used to analyse the anodic precipitate. Samples of the anodic precipitate for the analysis of XPS were placed in a bottle that was filled with argon gas to protect the sample from air oxidation.

2.2. *Reagents*

Reagent grade chemicals and ultrapure deionized water were used throughout the investigation.

2.3. *Experimental procedure*

The electrolytic solution was prepared by dissolving CuCN into NaCN + NaOH solution and then mixing with Na_2SO_4 solution to make the final solution. 100 cm^3 of the solution of the required composition were added to the electrolytic cell. The experiments were carried out under an argon atmosphere. The ohmic drop between the working electrode and the reference electrode was compensated by the current interruption technique. For each experiment, the electrode surface was first renewed using 600 grit sandpaper, polished with 4000 grit silicon carbide sandpaper and then soft tissue paper. Finally the disc surface was checked under a microscope for smoothness. To obtain a stable electrode condition and reproducible results, the electrode was first treated by cyclic voltammetry between 0 and 0.60 V vs SCE at 100 mV s^{-1} for 0.5 h and polarized repeatedly at 1 mV s^{-1} in the solution containing 0.25 M NaOH and 1 M Na_2SO_4 until the electrode reached a stable condition. The copper oxide film was deposited on the electrode by controlling the potential for a certain time. The time for the deposition of copper oxide depended on the particular equipment. 10 min was needed for studying the effect of copper oxide, 30 min for XPS and over 60 min for X-ray diffraction. The liquid junction potential was calculated by the Henderson equation [24] and the thermal liquid junction potential was measured using two calomel reference electrodes.

2.4. *Chemical analysis*

The total cyanide concentration was determined using the following distillation–absorption–titration procedure: (i) distillation of cyanide as HCN at a mildly acid pH of 4 in the presence of EDTA, (ii) absorption of HCN in 0.25 M NaOH solution, (iii) titration with silver nitrate. The copper concentration of copper cyanide solution was measured by oxidizing copper cyanide to cupric nitrate using concentrated nitric acid and titration with by EDTA. The amount of the copper in the copper oxide precipitated on the anode was measured by dissolving copper oxide into sulfuric acid and titration with EDTA. The anodic current efficiency of cyanide was determined by the change in the solution cyanide concentration using the above distillation–absorption–titration method. The anodic current efficiency for Cu(I) was determined by both measuring the initial and final concentrations in the solution after the electrolysis and measuring the amount of copper in the copper oxide precipitated during the coulometric measurements.

3. Results and discussion

3.1. *Polarization measurements and identification of the anodic precipitate*

Polarization measurements were conducted at 25, 40, 50 and 60 °C in alkaline solution with 1 M Na_2SO_4 supporting electrolyte and different concentrations of cyanide, copper and sodium hydroxide. As copper oxide

and hydroxide were precipitated on the electrode surface during the polarization measurements, the electrode surface was repolished after every polarization to ensure reproducible results. The polarization curves for 0.05 M cyanide and a CN:Cu mole ratio of 3 at 25, 40, 50 and 60 °C are shown in Figure 1. The anodic oxidation of copper cyanide can be divided into three reaction regions. In the first region (about 0–0.4 V vs SCE), no anodic precipitate was formed on the electrode. In the second stage (about 0.4–0.6 V vs SCE), the anodic precipitate was formed on the electrode surface and the current increased sharply with increasing potential. After the formation of the anodic precipitate, the current against potential was dependent on the temperature and the rotational speed. At 25 °C and 100 rpm, the current reached a limiting value and slightly changed with increasing potential. However, at a rotational speed $\geqslant$400 rpm, the current reached a maximum value and then decreased with increasing potential. At 40 °C and a rotational speed $\leqslant$1600 rpm and less, after the current reached a limiting value, it increased with increasing potential to some extent. At a rotational speed $\geqslant$2500 rpm, the current increased to a limiting value and decreased with increasing potential. At 50 and 60 °C, the current did not decrease with increasing potential. XPS analysis of the precipitate indicated that the precipitate was a combination of copper oxide and hydroxide. The content of CuO in the precipitate increased from about 50% at 25 °C to about 70% at 60 °C. The X-ray diffraction pattern of the precipitate was consistent with the XPS results. The increase in the content of CuO may be a cause for the change of the anodic behaviour of copper cyanide with temperature. From the cyclic voltammetry (Figure 2), the effect of the precipitation of copper oxide was also dependent on the potential applied. At 25 °C and 100 rpm, when the potential was swept from 0 to 0.55 V vs SCE and then back to 0 V vs SCE, the current for the negative-going sweep was larger than that for the positive-going sweep, meaning that the precipitate had a catalytic effect on the anodic oxidation of copper cyanide. When the potential was swept from 0 to 0.60 V vs SCE and then back to 0 V vs SCE, the current for the negative-going sweep was smaller than that for the positive-going sweep, meaning that the precipitate had a passivating effect on the anodic oxidation of copper cyanide. The change in the catalytic properties of copper oxide may be caused by the adsorption of oxygen. Figure 3 compares the rate of oxidation on either graphite or graphite coated with copper oxide. Figure 3 also provides a comparison

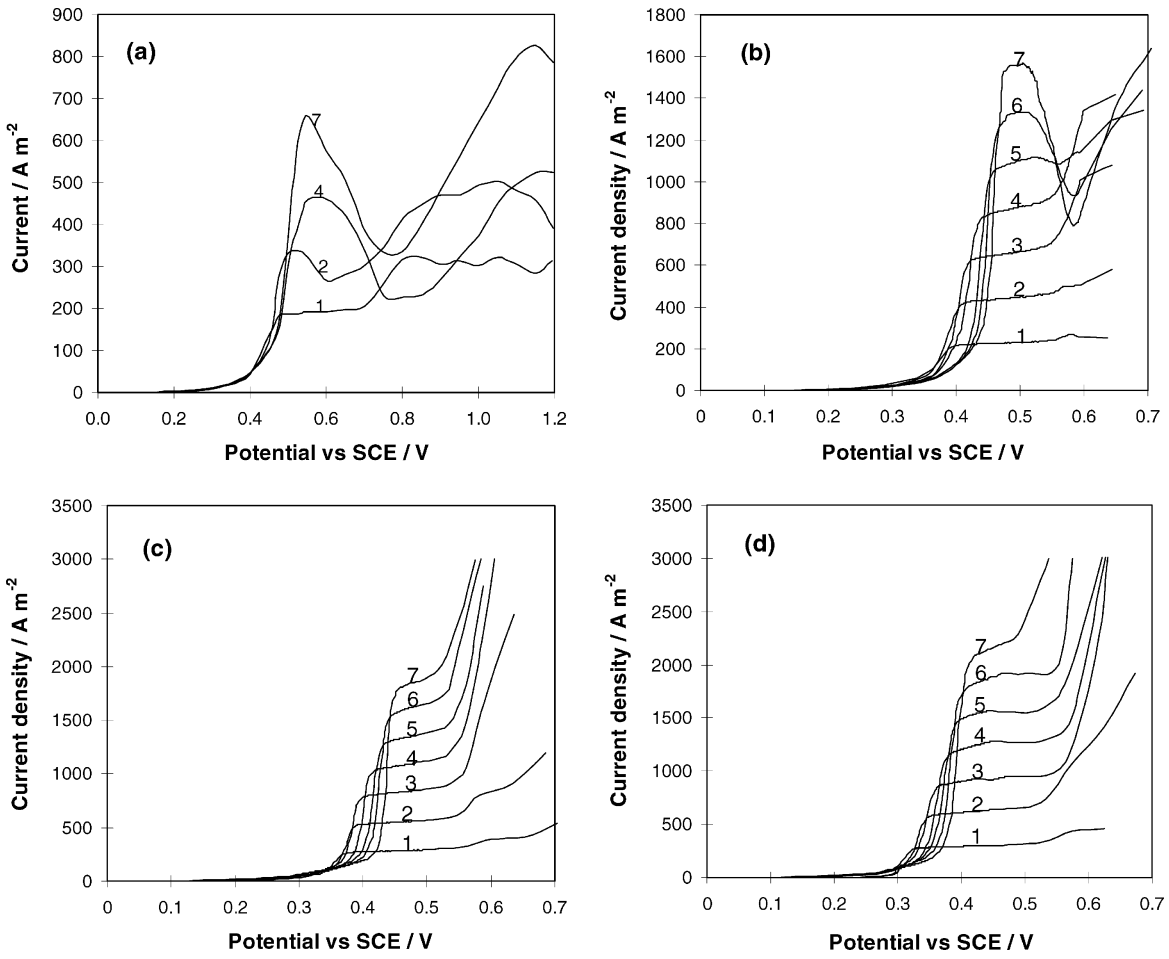

Fig. 1. Polarization curves for the anodic oxidaton of copper cyanide using a graphite rotating disc at (a) 25, (b) 40, (c) 50 and (d) 60 °C. Electrolyte: 0.05 M CN^-, CN:Cu = 3, 0.25 M NaOH, 1 M Na_2SO_4. Key: (1) 100, (2) 400, (3) 900, (4) 1600, (5) 2500, (6) 3600 and (7) 4900 rpm.

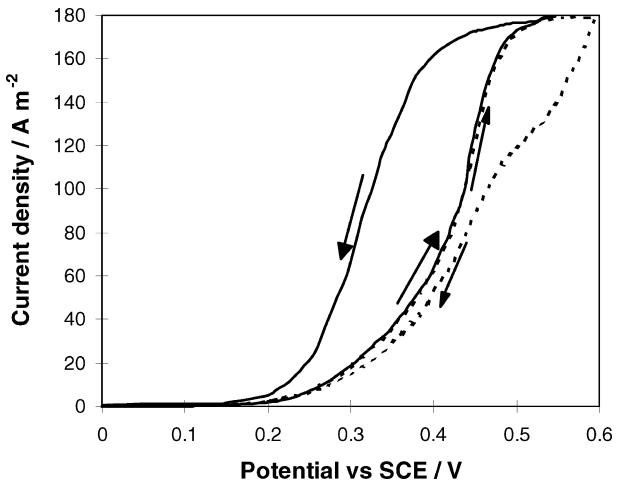

Fig. 2. Effect of the precipitated copper oxide on the oxidation of copper cyanide at 100 rpm and 25 °C: Electrolyte: 0.05 M CN^-, CN:Cu = 3, 0.25 M NaOH and 1 M Na_2SO_4. Key: (—) 0–0.55 and (- - -) 0–0.60 V vs SCE.

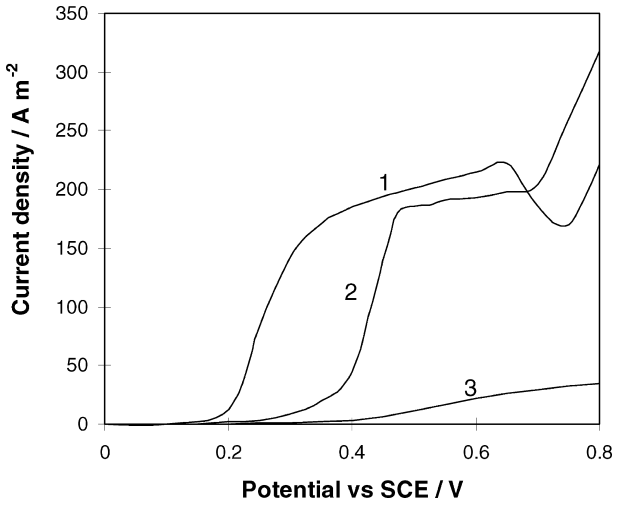

Fig. 3. Comparison of the effects of the precipitated copper oxide and copper ions on the anodic oxidation of cyanide on a graphite rotating disc at 100 rpm and 25 °C. Electrolyte: 0.25 M NaOH and 1 M Na_2SO_4. Key: (1) CuO coated graphite (0.05 M CN^-), (2) graphite (0.05 M CN^- and CN:Cu = 3) and (3) graphite (0.05 M CN^-).

between cyanide oxidation on graphite without copper in solution. The graphite anode coated with copper oxide apparently was the most catalytic system followed by graphite anode in a copper cyanide solution. Finally the graphite electrode immersed in a copper-free solution showed the slowest reaction. The precipitation of copper oxide and hydroxide suggests that copper cyanide can be oxidized to copper oxide and cyanate. Cyanide oxidation could be catalysed by the formation of cupric cyanide and cupric oxide.

The onset of the precipitation of copper oxide depends on the CN:Cu mole ratio and potential as discussed in Section 3.3. At a low rotational speed, the onset of the precipitation of copper oxide appeared at a lower potential than at high rotational, leading to a higher current, since copper oxide has a catalytic effect on cyanide. At a constant potential, the CN:Cu mole ratio at the electrode surface for a low rotational speed is lower than that at high rotational. The lowly coordinated copper cyanide complexes are less stable than the highly coordinated complexes and are easier to oxidize to copper oxide and cyanate. This results in the positive shift in the anodic curves with increasing rotational speed.

In the third region (potentials > about 0.6 V vs SCE), a gas was evolved, which could be oxygen or nitrogen due to the further oxidation of cyanate. In the absence of copper cyanide, the polarization curves on the electrode with precipitated copper oxide for the solution containing cyanate were almost the same as those without cyanate, suggesting that the evolution of oxygen was dominant.

3.2. *Coulometric measurement*

Controlled potential coulometry was used to determine the stoichiometry of the anodic oxidation of copper cyanide per faraday. The large rotating disc was used as an anode and the potential was controlled at values to minimize the rates of side reactions such as oxygen evolution. The working electrode (anode) was separated from the counter electrode (the cathode) to prevent the change of CN:Cu mole ratio due to copper deposition at the cathode. The results are listed in Table 1. Tests 1–4 show the amount of oxidized cyanide and copper(I) per faraday electricity at 0.05 M CN^-, a CN:Cu mole ratio of 3, 0.25 M NaOH and 1 M Na_2SO_4. If the reaction of the anodic oxidation proceeded according to the following reaction:

$$Cu(CN)_3^{2-} + 8OH^- = 3CNO^- + Cu(OH)_2 + 3H_2O + 7e^- \quad (19)$$

The amounts of oxidized cyanide and Cu(I) ion per faraday electricity are 0.429 and 0.143 mole, respectively. The corresponding values are close to the above values confirming the stoichiometry of Reaction 19. The current efficiencies for this reaction are 99.8, 102, 103, 105%, respectively, at 25, 40, 50 and 60 °C. Tests 5–9 show the amount of oxidized cyanide to copper per Faraday electricity at 0.05 M CN^-, a CN:Cu mole ratio of 4, 0.25 M NaOH and 1 M Na_2SO_4. Tests 5–8 were conducted at the potential where the current reached the limiting current at 100 rpm. Under the condition of tests 5–8, the reaction of the anodic oxidation approximately proceeds as the following reaction:

$$Cu(CN)_4^{3-} + 10OH^- = 4CNO^- + Cu(OH)_2 + 4H_2O + 9e^- \quad (20)$$

When the potential was controlled at a potential where no copper oxide formed (test 9), the amount of oxidized cyanide was 0.505 mol per faraday. The reaction can be expressed by the following reaction:

Table 1. Amount of oxidized cyanide and copper(I) per faraday at different CN:Cu mole ratio, hydroxide concentration and potentials

No.	Composition of solution	Temperature / °C	Potential vs SCE / V	Oxidized cyanide / mol F^{-1}	Oxidized copper / mol F^{-1}
1	0.05 M CN^-,	25	0.5	0.435	0.126
2	0.01667 M Cu^+	40	0.5	0.443	0.136
3	CN:Cu = 3	50	0.48	0.445	0.139
4	0.25 M NaOH	60	0.46	0.439	0.159
5	0.05 M CN^-,	25	0.5	0.447	0.102
6	0.0125 M Cu^+	40	0.5	0.449	0.106
7	CN:Cu = 4	50	0.48	0.467	0.110
8	0.25 M NaOH	60	0.46	0.470	0.110
9		25	0.3	0.505	0
10	0.05 M CN^-,	25	0.45	0.508	0
11	0.00417 M Cu^+	40	0.45	0.509	0
12	CN:Cu = 12	50	0.45	0.510	0
13	0.25 M NaOH	60	0.45	0.512	0
14	0.05 M CN^-,	25	0.6	0.510	0
15	0.00417 M Cu^+	40	0.6	0.511	0
16	CN:Cu = 12	50	0.6	0.512	0
17	0.01 M NaOH	60	0.6	0.515	0

$$CN^- + 2OH^- = CNO^- + H_2O + 2e^- \quad (21)$$

Tests 10–13 show the amount of oxidized cyanide to copper per faraday at 0.05 M CN^-, a CN:Cu mole ratio of 12, 0.25 M NaOH and 1 M Na_2SO_4. The amount of oxidized cyanide is very close to 0.5 mol per faraday (i.e., cyanide is oxidized to cyanate). When the concentration of hydroxide was 0.01 M NaOH, the amount of oxidized cyanide is still close to 0.5 mol per faraday (tests 14–17). Therefore, the stoichiometry of the anodic oxidation of copper cyanide mainly depends on the solution composition and potential.

3.3. *Effect of CN:Cu mole ratio*

The polarization curves for the anodic oxidation of copper cyanide with different CN:Cu mole ratios are given in Figure 4, showing that copper had a significant catalytic effect on cyanide oxidation. At a CN:Cu mole ratio of 3 and $[CN^-] = 0.05$ M, the anodic oxidation of copper cyanide began at 0.090, 0.045, 0.016 and 0.00 V vs SCE, respectively, for 25, 40, 50 and 60 °C. At a CN:Cu mole ratio $\geqslant 4$ and $[CN^-] = 0.05$ M, the anodic oxidation of copper cyanide began at 0.170, 0.145, 0.115, 0.085 V vs SCE respectively for 25, 40, 50 and 60 °C. The lower the mole ratio of cyanide to copper, the lower the potential for the onset of the formation of copper oxide. At a CN:Cu mole ratio of 3 and $[OH^-] > 0.05$ M, a small amount of copper oxide was even precipitated on the outer insulator. At a CN:Cu mole ratio greater than 3.5, there is no oxide precipitated on the outer insulator presumably due to copper(II) reduction in the cyanide-rich environment. When the CN:Cu mole ratio exceeded 6, no well-defined limiting current was obtained because oxygen was evolved before the current reached a limiting value.

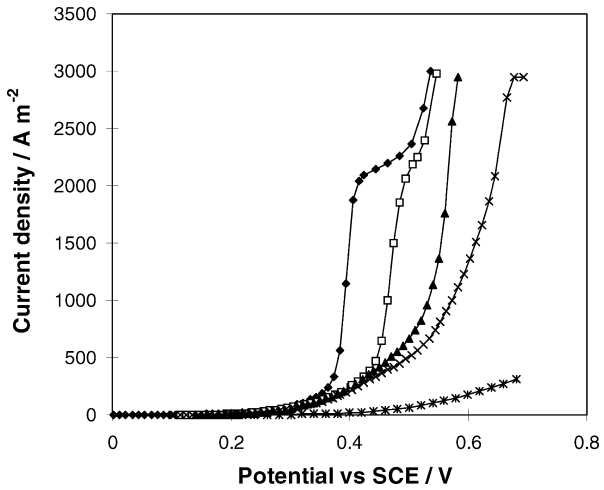

Fig. 4. Effect of copper ions on the anodic oxidation of cyanide. Current against potential on a graphite rotating disc at 4900 rpm and 60 °C. Electrolyte: 0.05 M CN^- with different CN:Cu mole ratios, 1 M Na_2SO_4 and 0.25 M NaOH. Key: (♦) CN:Cu = 3, (□) CN:Cu = 4, (▲) CN:Cu = 6, (×) CN:Cu = 12 and (✱) no Cu.

The plot of the potential against log current density at 4900 rpm is shown in Figure 5. Although no correction for the difference in the concentration between the bulk solution and the surface was made, at low potentials, the current was much lower than 10% of the limiting current. Thus the concentration difference can be neglected. When the concentration difference became significant, the formation of copper oxide began. At a CN:Cu mole ratio of 3, the Tafel slope was about 0.12 V $decade^{-1}$. At a CN:Cu mole ratio $\geqslant 4$, two Tafel slope ranges appear with the first Tafel slope being about 0.060 V $decade^{-1}$ and the second one about 0.18 V $decade^{-1}$. On a pyrolytic graphite rotating disc, there is only one well-defined Tafel slope at a CN:Cu mole ratio $\geqslant 4$ and the current for a CN:Cu mole ratio

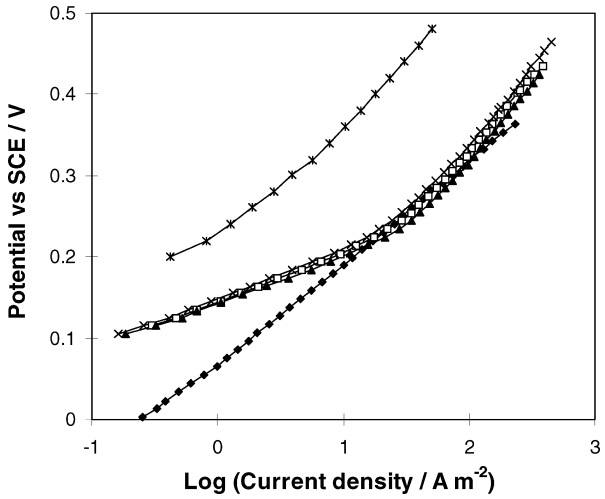

Fig. 5. Effect of copper on the anodic oxidation of cyanide. Potential against log (current density) on a graphite rotating disc at 4900 rpm and 60 °C. Electrolyte: 0.05 M CN^- with different CN:Cu mole ratios, 1 M Na_2SO_4 and 0.25 M NaOH. Key: (♦) CN:Cu = 3, (□) CN:Cu = 4, (×) CN:Cu = 6, (▲) CN:Cu = 12 and (✱) no Cu.

of 3 is larger than those with higher mole ratios of cyanide to copper. Therefore the anodic behaviour of copper cyanide is dependent on the anode materials. From Figure 5, at $[CN^-] = 0.05$ M, the current for a CN:Cu mole ratio of 4 (0.0125 M Cu^+) is even lower than that for a CN:Cu mole ratio of 6 (0.008 33 M Cu^+), but higher than that for a CN:Cu mole ratio of 12 (0.00467 M Cu^+). This is related to the change in the concentration of the discharged species (further discussed in the later section).

From Figure 6, at $[Cu^+] = 0.008\ 33$ M, when the cyanide concentrations increased from 0.025 to 0.4 M, the anodic behaviour of copper cyanide changed with cyanide concentration. At $[CN^-] = 0.025$ M (i.e., with a CN:Cu mole ratio of 3), the plot of the potential against log (current density) is a straight line. At $[CN^-] \geqslant 0.05$ M (i.e., CN:Cu mole ratio $\geqslant 6$), there are two Tafel slopes in the plots of the potential against log (current density). With increasing cyanide concentration, the curves for the plots of the potential against log (current density) are parallel to each other, but do not shift uniformly.

3.4. *Effect of pH*

From Figure 7, pH had a significant effect on the anodic oxidation of cyanide. At a CN:Cu mole ratio of 3, pH greatly affects the anodic oxidation of cyanide both at low and high potentials. At a low potential, the Tafel slope decreased from 0.130 to 0.060 V $decade^{-1}$ and the current decreased with decreasing pH at a constant potential. This suggests that the rate-controlling step changed or the mechanism changed. At a high potential, copper cyanide was oxidized to copper oxide and cyanate and the current was sensitive to the hydroxide concentration and the current did not reach a well-defined limiting value at low hydroxide concentration.

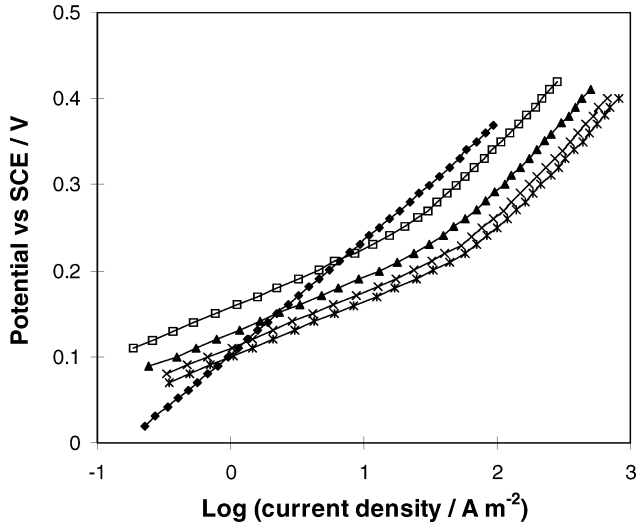

Fig. 6. Effect of copper on the anodic oxidation of cyanide. (a) Potential against log (current density) at 4900 rpm and 60 °C. Electrolyte: 0.008 33 M Cu with different CN^- concentrations, 1 M Na_2SO_4 and 0.25 M NaOH. Key: (♦) 0.025, (□) 0.05, (▲) 0.1, (×) 0.2 and (✱) 0.4 M CN^-.

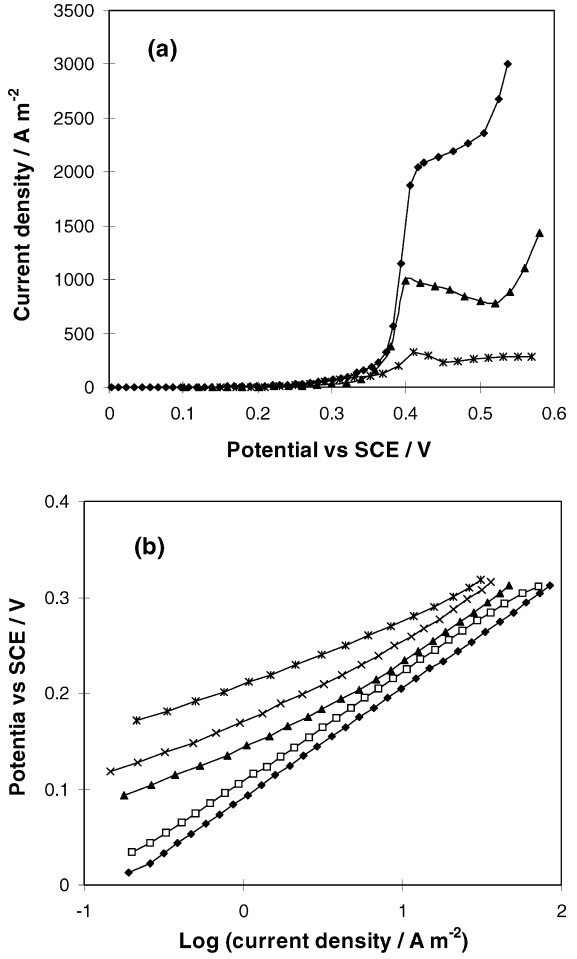

Fig. 7. Effect of pH on the anodic oxidation of cyanide. (a) Current density against potential and (b) potential against log (current density) on a graphite rotating disc at 4900 rpm and 60 °C. Electrolyte: 0.05 M CN^-, CN:Cu = 3 and 1 M Na_2SO_4. Key: (♦) 0.25, (□) 0.125, (▲) 0.05, (×) 0.025 and (✱) 0.01 M OH^-.

This means that hydroxide ions were involved in the rate-controlling step. Similar results were obtained on pyrographite and Pt rotating discs. At a CN:Cu mole ratio of 4 (Figure 8), at low potentials, the pH had little effect on the anodic oxidation of cyanide and the Tafel slope was independent of pH and the current decreased slightly with decreasing pH. This means that hydroxide was not involved in the rate-controlling step. At high potentials, copper cyanide was oxidized to copper oxide and cyanate and the current depends greatly on the hydroxide concentration. The higher the CN:Cu mole ratio, the less dependent was the current on the hydroxide concentration and the less copper oxide was formed. At a CN:Cu mole ratio of 12, and 0.01 M OH^{-1}, almost no copper oxide was precipitated on the electrode surface. Therefore the anodic oxidation of copper cyanide is a function of the CN:Cu mole ratio, cyanide concentration and pH.

3.5. *Reaction order*

To determine which of the copper cyanide species is discharged at the electrode surface, the reaction order with respect to various copper cyanide species was calculated by changing the copper cyanide concentration and the mole ratio of cyanide to copper and measuring the current against predicted concentration of copper cyanide species at a constant potential. The concentrations of copper cyanide species ($Cu(CN)_2^-$, $Cu(CN)_3^{2-}$ and $Cu(CN)_4^{3-}$) were calculated by solving the mass balance equations (Equations 17 and 18) related to Reactions 13–16. At a CN:Cu mole ratio of 3, the polarization curves were measured over the cyanide concentration range 0.025–0.2 M and the temperature range 25–60 °C. The current increased uniformly with increasing concentration of copper cyanide and the Tafel slope remained at about 0.120 V $decade^{-1}$. About 97% of the copper exists in the form of $Cu(CN)_3^{2-}$ and its concentration is proportional to the concentration of the total copper cyanide. The concentrations of CN^-, $Cu(CN)_2^-$ and $Cu(CN)_4^{2-}$ are very low and do not increase uniformly with increasing concentration of the total copper cyanide. The plots of log (current) against $\log([Cu(CN)_3^{2-}])$ at constant potentials gave straight lines having slopes 0.97–0.99 (Figure 9). This suggests that the reaction order with respect to tricyanide is one. Therefore $Cu(CN)_3^{2-}$ could be discharged at the electrode forming $Cu(CN)_3^-$. The same results were obtained on a pyrolytic graphite electrode. At 40, 50 and 60 °C, the same conclusions were reached.

From Figure 6, when the copper concentration was kept constant and the cyanide concentration increased from 0.05 to 0.4 M, the polarization curves shifted and were almost parallel to each other. This shift could be due to a change in the concentration of some copper cyanide species. The current at a constant potential was almost proportional to the concentration of $Cu(CN)_4^{3-}$ but not the other copper cyanide species. The plots of log (current) against $\log([Cu(CN)_4^{3-}])$ at 0.2 and 0.4 V vs SCE give straight lines having slopes of 0.96 and 1.1, respectively. The same results have been obtained when

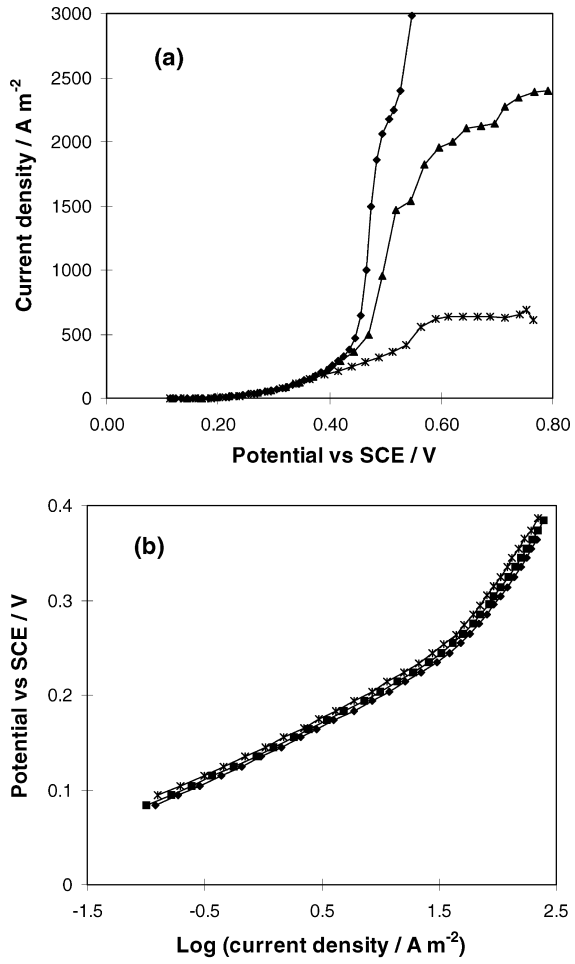

Fig. 8. Effect of pH on the anodic oxidation of cyanide. (a) Current density against potential and (b) potential against log (current density) on a graphite electrode at 4900 rpm and 60 °C. Electrolyte: 0.05 M CN^-, CN:Cu = 4, and 1 M Na_2SO_4. Key for (a): (♦) 0.25, (▲) 0.05 and (✱) 0.01 M $OH^-$and Key for (b): (♦) 0.25, (■) 0.05 and (✱) 0.01 M OH^-.

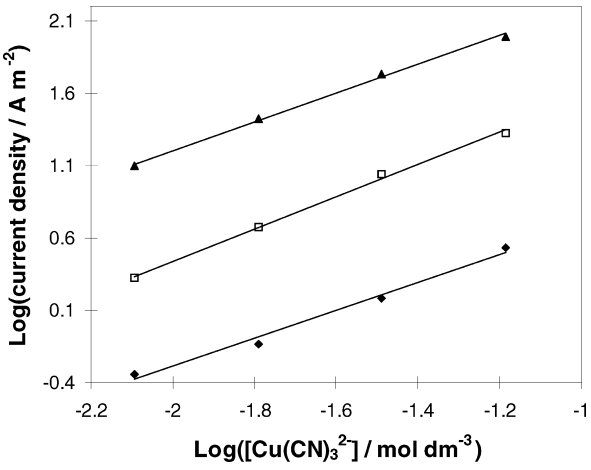

Fig. 9. Calculation of reaction order, log (current) against log (tricyanide concentration) on a graphite rotating disc at constant potentials, 4900 rpm and 25 °C. Electrolyte: 0.25 M NaOH, 1 M Na_2SO_4, CN:Cu mole ratio = 3. Key: (▲) 0.4, (□) 0.3 and (♦) 0.2 V vs SCE.

the total cyanide concentration was kept at 0.4 M and the copper concentration was changed. The reaction order with respect to $Cu(CN)_4^{3-}$ obtained on a pyrographite electrode was 1.0. Yoshimura et al. [7] thought that almost all of copper exists in the form of $Cu(CN)_4^{3-}$. They plotted the log (current) against log ($[Cu]_{Total}$) and obtained a slope of 0.9. However, from our calculation, only 68–76% of the copper exists in the form of $Cu(CN)_4^{3-}$ in the concentration range studied and the concentration of $Cu(CN)_4^{3-}$ is not exactly proportional to the total copper concentration. The plot of log ($[Cu(CN)_4^{3-}]$) against log ($[Cu]_{Total}$) gave a slope of 0.901. Therefore, the corrected reaction order with respect to $Cu(CN)_4^{3-}$should be 0.99 for [7]. From Figure 5, at $[CN^-] = 0.05$ M, the polarization curves for CN:Cu mole ratios = 4, 6, and 12 are very close and the current for a CN:Cu mole ratio of 6 ($[Cu] = 0.008\ 33$ M) at a constant potential is even larger than that for a CN:Cu mole ratio of 4 ($[Cu] = 0.0125$ M). This is because the concentration of $Cu(CN)_4^{3-}$ for a CN:Cu mole ratio of 6 is larger than that for a CN:Cu mole ratio of 4 and the current at constant potential is proportional to the concentration of $Cu(CN)_4^{3-}$.

The reaction order with respect to hydroxide was determined by changing the hydroxide concentration. From Figure 7, at a CN:Cu mole ratio of 3, the Tafel slope changes with hydroxide concentration and the rate-controlling step or the reaction mechanism change. From Figure 8, at a CN:Cu mole ratio of 4, the current only slightly changes with hydroxide concentration and the reaction order with respect to hydroxide is close to zero.

3.6. *Possible reaction mechanism*

3.6.1. *In the low potential region (< about 0.4 V vs SCE)*

At a CN:Cu mole ratio of 3 and $[OH^-] = 0.25$ M, $Cu(CN)_3^{2-}$ is discharged and oxidized to $Cu(CN)_3^-$ at the electrode.

With decreasing concentration of hydroxide, the current and the Tafel slope decreases and $Cu(CN)_3^{2-}$ becomes less electrochemically active. At $[OH^-] =$ 0.01 M, the Tafel slope decreases to 0.060 V decade^{-1}. This means that hydroxide ion affects the rate of $Cu(CN)_3^{2-}$ discharge.

As the CN:Cu mole ratio increases at a fixed cyanide concentration, the current and Tafel slope also decreases at low potentials. At CN:Cu > 4, there are two Tafel slopes with the first one being 0.060 V decade^{-1} and the second one about 0.17 V decade^{-1}. The discharged species shifts from $Cu(CN)_3^{2-}$ to $Cu(CN)_4^{3-}$. The reaction order with respect to hydroxide ion is almost zero.

At $[OH^-] = 0.01$ M and a constant potential, the ratio of the current measured in 0.05 M CN^- solutions with CN:Cu mole ratios of 3 and 4 is close to the mole ratio of $Cu(CN)_4^{3-}$ of the solutions. Therefore at CN:Cu = 3, with decreasing hydroxide concentration, the discharged species could shift from both $Cu(CN)_3^{2-}$ and $Cu(CN)_4^{3-}$ to only $Cu(CN)_4^{3-}$. At a high hydroxide concentration, $Cu(CN)_3^{2-}$ is discharged much faster than $Cu(CN)_4^{3-}$ and the current contributed by $Cu(CN)_4^{3-}$ can be neglected. With decreasing hydroxide concentration, the discharge of $Cu(CN)_3^{2-}$ is suppressed and the discharge of $Cu(CN)_4^{3-}$ maintains the constant rate and becomes the dominant discharged species. Increasing CN:Cu mole ratio will increase $Cu(CN)_4^{3-}$ and free CN^- and decrease $Cu(CN)_3^{2-}$ which also become less electrochemically active. Therefore, $Cu(CN)_4^{3-}$ becomes the dominant discharged species. From the above discussion, the following possible anode reactions are proposed:

At CN:Cu = 3 and a high concentration of hydroxide (0.25 M OH^-)

Step 1 $Cu(CN)_3^{2-} \rightarrow Cu(CN)_3^- + e^-$

Step 2 $2Cu(CN)_3^- \rightarrow 2Cu(CN)_2^- + (CN)_2$

Step 3 $(CN)_2 + 2OH^- \rightarrow CN^- + OCN^- + H_2O$

Step 1 could be the rate-controlling step from a Tafel slope of 0.12 V decade^{-1} [27] and the discharge of $Cu(CN)_4^{3-}$ is negligible compared to $Cu(CN)_3^{2-}$. Step 1 is enhanced by hydroxide ions. The rate of step 1 decreased with decreasing pH.

Increasing the mole ratio of cyanide to copper has a similar effect like decreasing pH because it shifts the distribution of copper cyanide species from lowly coordinated complexes to highly coordinately complex ($Cu(CN)_4^{3-}$) and suppresses the discharge of $Cu(CN)_3^{2-}$. The critical value for CN:Cu depends on the total copper cyanide concentration because the distribution of copper cyanide species is dependent on cyanide concentration. For example, at $[CN^-] =$ 0.05 M and $[OH^-] = 0.25$ M when CN:Cu > about 4, the discharge of $Cu(CN)_4^{3-}$ is dominant. However, at $[CN^-] = 3$ M and $[OH^-] = 0.25$ M, when CN:Cu $\geqslant$ 3.5, the discharge of $Cu(CN)_4^{3-}$ become dominant.

When the dominant discharged species is $Cu(CN)_4^{3-}$, the anodic reaction can probably be modelled by the following steps:

Step 1 $Cu(CN)_4^{3-} \underset{k_{-1}}{\overset{k_1}{\Leftrightarrow}} Cu(CN)_{4(ads)}^{2-} + e^-$

Step 2 $Cu(CN)_{4(ads)}^{2-} \underset{k_{-2}}{\overset{k_2}{\Leftrightarrow}} Cu(CN)_4^{2-}$

Step 3 $2Cu(CN)_4^{2-} \rightarrow 2Cu(CN)_3^{2-} + (CN)_2$

Step 4 $(CN)_2 + 2OH^- \rightarrow CNO + CN^- + H_2O$

The adsorption rate for the coverage of $Cu(CN)_4^{2-}$ ($d\theta/dt$) can be expressed as the following equation:

$$\frac{d\theta}{dt} = k_1(1-\theta)[Cu(CN)_4^{3-}] - k_{-1}\theta - k_2\theta + k_{-2}(1-\theta)[Cu(CN)_4^{2-}] \quad (22)$$

where θ is the coverage of $Cu(CN)_4^{2-}$ on the electrode, α the charge transfer coefficient, k_1 the rate constant for the electrochemical adsorption, k_{-1} the rate constant for the electrochemical desorption, k_2 the rate constant for the chemical desorption and k_{-2} the rate constant for the chemical adsorption.

At steady-state, $d\theta/dt = 0$ and if $\theta \approx 0$ and the chemical adsorption of $Cu(CN)_4^{2-}$ is negligible, the following equation can be obtained from Equation 22:

$$\theta = \frac{(k_1/k_{-1})[Cu(CN)_4^{3-}]}{1 + k_2/k_{-1}} = \frac{(k_{0,1}/k_{0,-1})[Cu(CN)_4^{3-}]\exp(FE/RT)}{1 + (k_2/k_{0,-1})\exp((1-\alpha)FE/RT)} \quad (23)$$

$$i = Fk_2\theta = \frac{F(k_2k_{0,1}/k_{0,-1})[Cu(CN)_4^{3-}]\exp(FE/RT)}{1 + (k_2/k_{0,-1})\exp((1-\alpha)FE/RT)} \quad (24)$$

where α is the charge transfer coefficient, $k_{0,1}$ and $k_{0,-1}$ is the rate constants, respectively, for oxidation and reduction, $k_1 = k_{0,1}\exp(\alpha FE/RT)$ and $k_{-1} = k_{0,-1}\exp(-(1-\alpha)FE/RT)$. From Equation 24, the reaction order with respect to $Cu(CN)_4^{2-}$ is one at any potential.

In the initial low potential region, if $k_{-1} \gg k_2$, the following equation can be obtained:

$$i = Fk_2\theta = \frac{Fk_2k_{0,1}}{k_{0,-1}}[Cu(CN)_4^{3-}]\exp\left(\frac{FE}{RT}\right) \quad (25)$$

From Equation 25, the Tafel slope is RT/F (about 0.06 V decade^{-1}). Therefore, the above assumption is consistent with the experimental results.

When the potential increases to a value where k_{-1} is $\ll k_2$, from Equation 24, the coverage of the adsorbed $Cu(CN)_4^{2-}$ can be expressed as

$$i = Fk_2\theta = Fk_1[Cu(CN)_4^{3-}] = Fk_{0,1}[Cu(CN)_4^{3-}]\exp\left(\frac{\alpha FE}{RT}\right) \quad (26)$$

From the above equation, the reaction order with respect to $Cu(CN)_4^{3-}$ is one and Tafel slope is $RT/\alpha F$. This is consistent with the experiment results. From the plot of log (current density) against the potential (or the potential against log (current density) according to Equations 25 and 26, we can calculate $Fk_2k_{0,1}\times[Cu(CN)_4^{3-}]/k_{0,-1}$ and $Fk_{0,1}[Cu(CN)_4^{3-}]$ which can be used to model and predict the kinetics process. Figure 10 shows the plots of potential against log (current density) using data measured and predicted using Equation 24. The predicted data are generally consistent with data measured at the potential < 0.45 V vs SCE. On a pyrolytic graphite, the adsorption of $Cu(CN)_4^{2-}$ is probably so low that its effect can be neglected and therefore only the second Tafel slope was observed.

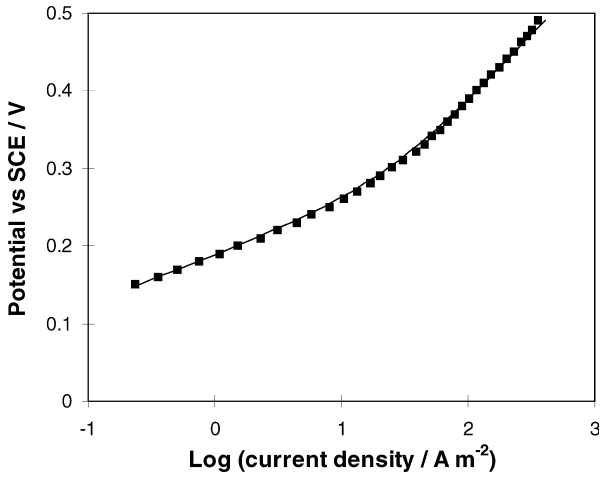

Fig. 10. Potential against log (current density) on a graphite rotating disc using data measured and predicted using Equation 24 (constants used was determined by the measured data) at 4900 rpm and 25 °C. Electrolyte: 0.1 M CN^-, CN:Cu = 12, 0.25 M NaOH and 1 M Na_2SO_4. Key: (—) predicted and (■) measured.

3.6.2. *In the high potential region (>about 0.4 V vs SCE)* In this region copper oxide or hydroxide is precipitated on the anode. At CN:Cu around 3, a small amount of copper oxide was precipitated on the outer insulator. This suggests that some of $Cu(CN)_3^-$ generated at the anode may diffuse to the surface of the outer insulator and decompose to form copper oxide.

The effect of the precipitated copper oxide on the anodic oxidation of copper cyanide depends on the applied potential, temperature and total cyanide concentration. At $[CN^-] = 0.05$ M and temperature above 40 °C, copper oxide significantly catalyses the oxidation of copper cyanide, at temperature below 40 °C copper oxide has limited catalytic effect on the cyanide oxidation or even exhibits the inhibiting effect at the potential >0.6 V vs SCE. The free cyanide oxidation was catalysed by cupric oxide formed on the electrode because in the absence of copper, the anodic current of free cyanide on copper oxide-coated anode is significantly higher than on the anode without copper oxide. The solubility of copper(II) (CuO) is 10^{-6} M in the form of CuO_2^- at 25 °C in 0.25 NaOH solution and therefore the effect of the soluble Cu(II) on the cyanide oxidation is not considered. Cu(III) species such as Cu_2O_3 can be produced in the potential range studied [28–30]. For example, Cu(III) oxide phase was stabilized at approximately 0.48 V vs SCE and 0 °C in alkaline solution [28], the oxidation of Cu(II) species began at about 0.35 V vs SCE and 24 °C in 1 M NaOH [29] and the intrinsic redox potential for Cu(III)/Cu(II) in the solid oxide is 0.42 V vs SCE at pH 14 at 20 °C [30]. It is possible for Cu(III) to form on the surface and catalyze cyanide oxidation as was suggested by Wells and Johnson [15]. The reaction procedure could be expressed by the following reaction:

Step 1 $Cu(CN)_n^{-(n-1)} \longrightarrow Cu(CN)_{n(ads)}^{-(n-2)} + e^-\ (n = 2, 3, 4)$

Step 2 $Cu(CN)_{n(ads)}^{-(n-2)} + 2OH^- \longrightarrow nCN_{(ads)}^- + Cu(OH)_2$ (or $CuO + H_2O$)

Step 3 $Cu(CN)_n^{-(n-1)} \longrightarrow Cu(CN)_n^{-(n-2)} + e^-$

Step 4 $Cu(CN)_n^{-(n-2)} = Cu(CN)_{(n-1)}^{-(n-2)} + \frac{1}{2}(CN)_2$

Step 5 $CN_{(ads)}^- + 2OH^- \xrightarrow{\text{Catalyzed by copperoxide}} CNO^- + H_2O$

With decreasing pH and increasing mole ratio of cyanide to copper, step 1 ($n = 2$ and 3), step 2, step 3 ($n = 2$ and 3) and step 5 are suppressed. This results in a decrease in the current and it is in agreement with the experiment results. At a high CN:Cu ratio and low pH, no copper oxide is formed.

3.7. *Diffusion coefficient estimation*

In the presence of a large amount of supporting electrolyte, the limiting current for a simple electrochemical reaction ($O + ne^- = R$) on the rotating disc can be expressed by the Levich equation:

$$i_l = 0.62\, nFD^{2/3}v^{-1/6}\omega^{1/2}C_b \qquad (27)$$

where n is the number of the electrons transferred, F the faradaic constant, D the diffusion coefficient, v the kinematic viscosity, ω the rotational speed and C_b the bulk solution concentration. The diffusion coefficients can be calculated from the slopes of the straight lines for the plots of i_l against $\omega^{1/2}$. At CN:Cu = 3, when the current is the limiting region, the anodic reaction can be expressed as Reaction 20, which can be used to estimate the number of electrons transfered per one tricyanide. The plots of the limiting current against $\omega^{1/2}$ for 0.05 M CN^- and CN:Cu = 3 gives a straight line. At CN:Cu = 3, 97% of copper and cyanide exists in the form of $Cu(CN)_3^{2-}$ and the calculated diffusion coefficient can be assumed to be those of $Cu(CN)_3^{2-}$. The diffusion coefficients for $Cu(CN)_3^{2-}$ at 40, 50 and 60 °C were found to be 1.05×10^{-9}, 1.29×10^{-9} and 1.52×10^{-9} $m^2\ s^{-1}$. The diffusion activation energy is 16.6 kJ mol^{-1}. From the activation energy, the predicted diffusion coefficient at 25 °C is 0.76×10^{-9} $m^2 s^{-1}$.

4. Conclusions

(i) Copper has a significant catalytic effect on cyanide oxidation. Generally, the anodic oxidation of copper cyanide can be divided into three reaction regions. In the low potentials region (roughly, 0–0.4 V vs SCE), cuprous cyanide is oxidized to cupric cyanide complexes which produce cyanogen, which in turn reacts with hydroxide to form cyanate. In the middle potential region (roughly, 0.4–0.6 V vs SCE), copper oxide is precipitated on the electrode. Copper cyanide is oxidized to copper oxide and cyanate. The potential for the precipitation of copper oxide is dependent on the mole ratio of cyanide to copper and temperature. The higher the mole ratio of cyanide to copper, the higher the potential for the precipitation of copper oxide.

(ii) The electrochemical kinetic behavior is dependent on the CN:Cu mole ratio, pH and total cyanide concentration. At CN:Cu = 3 and $[OH^-] = 0.25$ M, the Tafel slope is about 0.12 V $decade^{-1}$ and the reaction order with respect to $Cu(CN)_3^{2-}$ is one. $Cu(CN)_3^{2-}$ is discharged on the electrode. The current and Tafel slope decrease with decreasing hydroxide concentration and so hydroxide is involved in the rate-determining step. With increasing mole ratio of cyanide to copper, the anodic behaviour of copper cyanide changes. When the mole ratio of cyanide to copper is larger than a certain value (about 4 at $[CN^-] = 0.05$ M), a Tafel slope of about 0.06 V $decade^{-1}$ was observed over the potential (0.1–0.25 V vs SCE) and a second Tafel slope of about 0.18–0.20 V $decade^{-1}$ over the higher potential range. This change is related to the change in the distribution of copper cyanide species which results in the shift of the discharged species to $Cu(CN)_4^{3-}$.

References

1. G.H. Clevenger and M.I. Hall, *Trans. Am. Electrochem. Soc.* **24** (1914) 271.
2. D.T. Sawyer and R.J. Day, *J. Electroanal. Chem.* **5** (1963) 195.
3. A.T. Kuhn, *J. Appl. Chem. Biotechnol.* **21** (1972) 29.
4. J.J. Byerley and K. Enns, U.S.N.I.T.S., A.D. Rep. PB235588 (1974), pp. 1–49.
5. S. Yoshimura, A. Katagiri, Y. Deguchi and S. Yoshizawa, *Bull. Chem. Jpn.* **53** (1980) 2434.
6. S. Yoshimura, A. Katagiri, Y. Deguchi and S. Yoshizawa, *Bull. Chem. Jpn.* **53** (1980) 2437.
7. A. Katagiri, S. Yoshimura, Y. Deguchi and S. Yoshizawa, *in* W.E. O'Grady et al. (Eds), The Proceedings of the Symposium on Electrocatalysis, (PV 82-2) (1982), pp. 336–346.
8. M.C. Dart, J.D. Jentles and D.G. Renton, *J. Appl. Chem.* **13** (1963) 55.
9. J. Drogen and L. Pasek, *Plat. Surfa. Finish.* **18** (1964) 310.
10. S. Ehdaie, M. Fleischmann and R.E.W. Jansson, *J. Appl. Electrochem.* **12** (1982) 75.
11. T.C. Tan, W.K. TEO and D-T. Chin, *Chem. Eng. Commun.* **38** (1985) 125.
12. F. Hine, M. Yasuda, T. Iida and Y. Ogata, *Electrochim. Acta* **31** (1986) 1389.
13. J. Hwang, Y. Wang and C. Wan, *J. Appl. Electrochem.* **17** (1987) 684.
14. N.L. Piret and H.J. Schippers, 'Extraction Metallurgy 89' (1989), pp. 1041–1080.
15. B. Wells and D.C. Johnson, *J. Electrochem. Soc.* **137** (1990) 2785.
16. M.L. Lin, Y.Y. Wang and C.C. Wan, *J. Appl. Electrochem.* **22** (1992) 1197.
17. C.S. Hofseth and T.W. Chapman, *J. Electrochem. Soc.* **139** (1992) 2525.
18. D.B. Dreisinger, J. Ji and B. Wassink, The Proceeding of Randol Gold Forum, Perth (1995), pp. 239–244.
19. D.B. Dreisinger and J. Lu, unpublished results (1997).
20. J. Lu, D.B. Dresinger and W.C. Cooper, *J. Appl. Electrochem.* (1999) 1161.
21. R.M. Izatt, H.D. Johnston, G.D. Watt and J.J. Christensen, *Inorg. Chem.* **6** (1967) 132.
22. M.T. Beck, *Pure Appl. Chem.* **59** (1987) 1703.
23. J. Lu, D.B. Dresinger and W.C. Cooper, *Hydrometallury*, in press.
24. P. Henderson, *Z. Phys. Chem.* **59** (1907) 118 and **63** (1908) 325.
25. A.G. Sharpe, 'The Chemistry of Cyano Complexes of the Transition Metals' (Academic Press, London, 1976), pp. 271–272.
26. O. Monsted and J. Bjerrum, *Acta Chem. Scand.* **21** (1967) 116.
27. J.O'M. Bockris and A.K.N. Reddy, *in* 'Modern Electrochemistry', Vol. 2, (Plenum Press, New York, 1970), chapter 9.
28. R. Dolhez, *Bull. Soc. R. Sci. Liege* **30** (1961) 446.
29. B. Miller, *J. Electrochem. Soc.* **116** (1969) 1675.
30. F. Beck and U. Barsch, *J. Electroanal. Chem.* **282** (1990) 175.